THE JOURNAL OF PHYSICAL CHEMISTRY B

Article

pubs.acs.org/JPCB

Understanding Selectin Counter-Receptor Binding from Electrostatic Energy Computations and Experimental Binding Studies

Anna Lena Woelke,[†] Christian Kuehne,[‡] Tim Meyer,[†] Gegham Galstyan,[†] Jens Dernedde,[‡] and Ernst-Walter Knapp*,[†]

[†]Institute of Chemistry and Biochemistry, Freie Universität Berlin, D-14195 Berlin, Germany

[‡]Charité-Universitätsmedizin Berlin, Klinische Chemie und Pathobiochemie, D-12200 Berlin, Germany

Supporting Information

ABSTRACT: Higher organisms defend themselves against invading micro-organisms and harmful substances with their immune system. Key players of the immune system are the white blood cells (WBC), which in case of infection move in an extravasation process from blood vessels toward infected tissue promoting inflammation. This process starts with the attachment of the WBC to the blood vessel wall, mediated by protein pair interactions of selectins and counter-receptors (C-R). Individual selectin C-R binding is weak and varies only moderately between the three selectin types. Multivalency enhances such small differences, rendering selectin-binding type specific. In this work, we study selectin C-R binding, the initial step of extravasation. We performed electrostatic energy computations based on the crystal structure of one selectin type co-crystallized with the ligating part of the C-R. The agreement with measured free energies of binding is satisfactory. Additionally, we modeled selectin mutant structures in order to explain differences in binding of the different selectin types. To verify our modeling procedures, surface plasmon resonance data were measured for several mutants and compared with computed binding affinities. Binding affinities computed with soaked rather than co-crystallized selectin C-R structures do not agree with measured data. Hence, these structures are inappropriate to describe the binding mode. The analysis of selectin/C-R binding unravels the role played by individual molecular components in the binding event. This opens new avenues to prevent immune system malfunction, designing drugs that can control inflammatory processes by moderating selectin C-R binding.

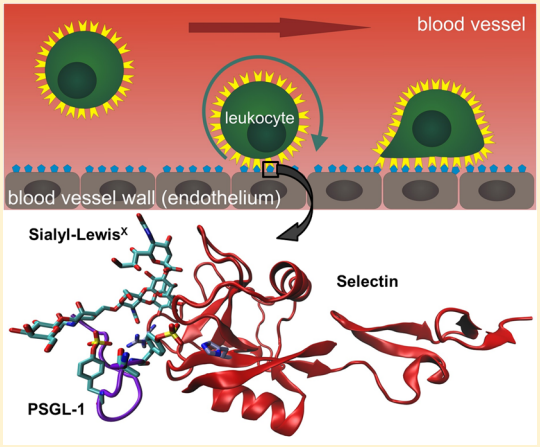

INTRODUCTION

The immune system protects an organism against invading micro-organisms and foreign substances that may infect tissue and ultimately cause diseases. It consists of a network of cells and tissues, which conduct the immune response in infected tissues through complex concerted processes. Major players of the immune system are the white blood cells (leukocytes) that circulate between blood, lymphatic, and surrounding tissues. Leukocytes are able to emigrate from blood vessels to reach lymph nodes or infected tissues. Such extravasation events start with tethering and rolling of leukocytes on the blood vessel wall, which slows down their motion in the bloodstream[1,2] (see our TOC figure). The transient attachments of leukocytes to the endothelial wall of blood vessels are mediated by pairwise binding processes between selectins and glycoproteins being their counter-receptors (C-R). Up-regulated selectin production may cause autoimmune diseases and is involved in tumor cell metastasis, while down-regulation may cause recurrent bacterial infection and persistent inflammation.[3] Therefore, selectin C-R interaction is considered as an interesting drug target.[4−6]

The selectin C-R binding interaction is in the range of a few tens of kJ/mol, which is rather small for the size of the participating molecular components. Despite this, such interactions can trigger dramatic processes due to a cooperative enhancement effect. Leukocytes possess thousands of selectins on their cell surface and can therefore simultaneously interact with many C-R, localized on the endothelial surface of the blood vessel, giving rise to much stronger multivalent interactions.[7]

Multivalent binding effects, involved in leukocyte attachment to blood vessel walls, have a double function. (1) Since individual pairwise selectin C-R binding interactions are weak, a few such interactions will not trigger an inflammatory process. This threshold effect renders extravasation error-prone. (2) Subtle differences in selectin C-R binding are enhanced by the multivalent effect,[8,9] which is governed by variations in individual binding strengths and abundance of available binding partners on leukocyte and endothelial surfaces. Thus, the multivalent effect can establish type-specific selectin C-R binding, even though the differences in binding affinities of individual selectin C-R pairs are small.

Received: October 6, 2013
Revised: December 2, 2013
Published: December 4, 2013

dx.doi.org/10.1021/jp4099123 | J. Phys. Chem. B 2013, 117, 16443−16454

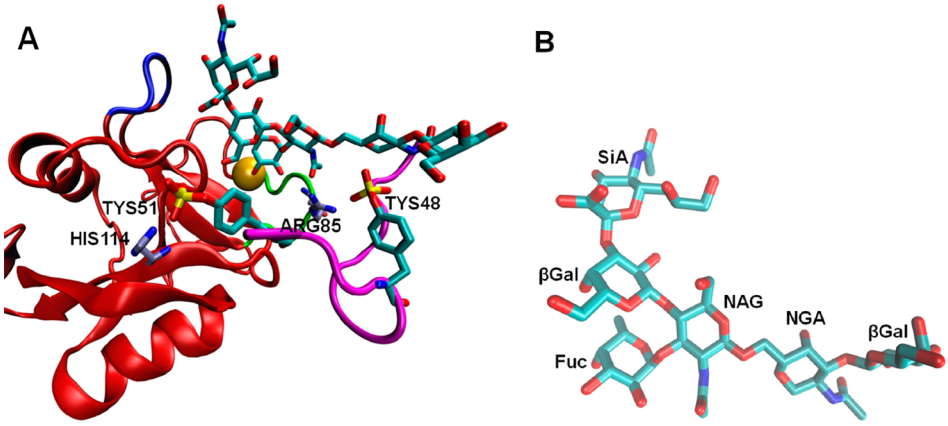

Figure 1. (A) Crystal structure of the lectin domain, the binding portion of P-selectin, co-crystallized with the binding part of the C-R, the PSGL-1 ligand (PDB id 1G1S) (11). P-selectin (red) and PSGL-1 peptide (magenta) are depicted as a rubber band model. The variable loop involving residues 83−89 of P-selectin is depicted in green; the sialic acid (SiA) binding loop (97−100) is depicted in dark blue. For crystallization, the calcium atom of selectin was replaced by strontium (yellow sphere). The carbohydrate part of the PSGL-1 ligand and the residues involved in salt-bridges (TyS48/His114 and TyS51/Arg85) are shown explicitly as stick models. (B) Structure of the hexasaccharide (SLe^X, NGA, and βGal) attached to the PSGL-1 ligand part of C-R. It consists of two branches: the tetrasaccharide Sialyl-Lewis^X (SLe^X), composed of the monosaccharides fucose (Fuc), *N*-acetylglucosamine (NAG), β-galactose (βGal), sialic acid (SiA) and the two saccharides *N*-acetylgalactosamine (NGA) and βGal that are connecting SLe^X with the polypeptide part of PSGL-1 depicted as a magenta rubber band in part A.

There are three types of selectins, platelet and endothelial cell (P), leukocyte (L), and endothelial cell (E) selectins, that are named according to the cell type they are mainly expressed by.[3] All three types of selectins possess the same domain structure. The N-terminal lectin domain interacts directly with the C-R. This domain exhibits sequence identities of more than 50% and possesses the same three-dimensional structure for all three selectin types. It is thus not surprising that these selectins have similar binding specificities.

In particular, the P-selectin glycoprotein ligand-1 (PSGL-1) is a relevant C-R for all three types of selectins.[10] PSGL-1 is post-translationally modified by glycosylation—attaching the so-called Sialyl-Lewis^X (SLe^X) tetrasaccharide—and by sulfation of tyrosine residues near the N-terminus. It is this part—called henceforth the PSGL-1 ligand—that binds to the lectin domain of selectins. Although a co-crystallized structure of P-selectin with the PSGL-1 ligand has been available[11] (Figure 1) for more than 10 years, the specificity of selectin PSGL-1 ligand binding is far from being understood.

In this work, we investigate the binding properties of the three types of selectin with the PSGL-1 ligand and the SLe^X tetrasaccharide motif alone. We compare binding free energies obtained by electrostatic energy computations with available data on binding affinities.[12−15] The binding behavior of several specific point mutations is verified experimentally using surface plasmon resonance (SPR) and compared with computed binding affinities.

Computing meaningful binding free energies for such complex molecular systems is a challenge, since the net total interactions are of moderate strength (50 kJ/mol or even smaller) and vary only slightly between selectin types. To the best of our knowledge, this is the first systematic analysis of selectin ligand binding covering in detail all three types of selectins and all regions of binding. A complete knowledge of the molecular basis of these interactions is the key to understanding the initial phase in immune response.

MATERIALS AND METHODS

Crystal Structures of Selectins. The atomic coordinates of selectins and selectin ligand complexes were taken from the Protein Data Bank (PDB).[16] They are based on crystal structures that include both the lectin and epidermal growth factor domains of selectin. For P-selectin, two crystal structures complexed with different ligating units are available. One is co-crystallized with the complete ligating unit of PSGL-1 (PDB id 1G1S),[11] and the second is soaked with SLe^X (PDB id 1G1R),[11] which is only part of the ligating unit. For E-selectin, only a crystal structure soaked with SLe^X is available (PDB id 1G1T),[11] while for L-selectin only an uncomplexed crystal structure is available (PDB id 3CFW).[17] Thus, for L-selectin, we add the ligand by modeling as described below. Hydrogen atoms were added by energy minimization, fixing all other atoms at their crystal structure positions using CHARMM.[18] The crystal structures and the modeled structures of the different selectins complexed with the PSGL-1 ligand unit used in the present study are listed in Table S1 of the Supporting Information.

Structural Adjustments and Force Field Used for Selectin Ligand Complexes. Modeling and energy minimizations were performed with CHARMM[18,19] using a combination of the CHARMM22 force field[20,21] with the CHARMM36 extension for carbohydrates.[22,23] Lacking force field parameters (in particular for the carbohydrate part of the ligand and the tyrosine sulfates) were created using existing parameters of similar compounds. The strontium ion in the 1G1S crystal structure was replaced by calcium, and the ligating amino acid side chains were adjusted by local energy minimization to take account of the smaller calcium radius. To allow for appropriate calcium−oxygen distances, the calcium ion radius was chosen to be 1.5 Å. Short hydrogen bonds with heteroatom distances below 2.6 Å occurring in the crystal structures were geometry optimized by local energy minimizations.

Atomic partial charges of standard amino acids were adopted from the all-atom CHARMM22[20,21] parameter set. Lacking partial charges for carbohydrates and tyrosine sulfates were determined with quantum chemical calculations (see below). Protonation states of titratable residues were determined using the software karlsberg+[24,25] (see below).

Computation of Partial Charges for Sialyl-Lewis^X Ligand and Tyrosine Sulfates. Density functional theory

dx.doi.org/10.1021/jp4099123 | J. Phys. Chem. B 2013, 117, 16443−16454

(DFT)[26,27] computations with Jaguar v7.7[28] using the B3LYP functional[29−32] and 6-31G** basis set[33−35] were performed for the individual monomeric saccharides and sulfated tyrosines in order to calculate atomic partial charges. To obtain the atomic charges at the atoms where the monomeric saccharides are connected, we performed such computations exemplary for the dimer NAG-Fuc. Atomic coordinates were extracted from the crystal structure of P-selectin with PSGL-1 ligand (PDB id 1G1S).[11] Bond lengths and angles were optimized keeping torsion angles fixed. Atomic partial charges were generated with RESP[36,37] using the quantum chemically computed electrostatic potential in the neighborhood of the molecule. Atomic coordinates and partial charges of the saccharide monomers and the sulfated tyrosine are given in Table S2 of the Supporting Information.

Modeling Structures of Selectin in Complex with PSGL-1 Ligand. A crystal structure complexed with the ligating part of PSGL-1 is available only for P-selectin (PDB id 1G1S),[11] but it contains no atomic coordinates of the side chain of the sulfated tyrosine TyS46. Hence, the atomic coordinates of this side chain were modeled. The resulting structure shows a solvent-exposed TyS46 of the ligand, which can then bind Lys8 and Lys112 via weak salt-bridges. The tertiary structures of the different selectins are very similar except for a loop comprising residues 83−89 that we define as a "variable loop" (magenta band in Figure 1A). Therefore, this P-selectin structure was used as a template to model the corresponding structures of L- and E-selectin. For this purpose, L-selectin was pairwise-structure aligned with the complex of P-selectin and PSGL-1 ligand using the backbone atoms of the three central β-strands (residues 49−51, 90−94, and 103−107) that form the interface of selectin with the PSGL-1 ligand. The resulting coordinates of the PSGL-1 ligand were transferred to the L-selectin crystal structure with no ligand. For E-selectin, the structure alignment was performed involving the fucose (Fuc) monomer present in the E-selectin soaked structure (1G1T). The PSGL-1 ligand of the P-selectin complex was then transferred to the E-selectin structure without ligand analogously to L-selectin.

Subsequently, the interface residues of L- and E-selectins were pulled toward the template positions in the P-selectin structure by constrained energy minimization of local parts of the structure to form appropriate salt-bridges and hydrogen bonds. For the L-selectin complexed with PSGL-1 ligand, the residues 78−89 of a loop regime (including the variable loop, Figure 1A), the attached calcium ion, and residue Lys8 were pulled toward their corresponding position in P-selectin such that the two salt-bridges $TyS46_{PSGL\text{-}1}/Lys8_{L\text{-}selectin}$ and $TyS51_{PSGL\text{-}1}/Lys85_{L\text{-}selectin}$ were formed. Lys84 was pulled out of the interface to prevent side chain clashes with SLe^X.

An analogue procedure with constrained energy minimization was applied for E-selectin complexed with the PSGL-1 ligand, where the calcium ion and the residues 83 and 88 were pulled toward their positions found in P-selectin. In addition, the hydrogen bond between fucose and $Glu107_{E\text{-}selectin}$ was forced to form. The short H-bonds between selectin and the fucose and galactose monomers that resulted from the pulling procedure were healed by local energy minimization. Since E-selectin shows no significant difference in binding affinities of PSGL-1 with or without the sulfated tyrosines,[38,39] the peptidic part of PSGL-1 was pulled away from E-selectin in the structure used for electrostatic energy computations.

After these modeling steps, all residues in the binding interface were energy minimized for L- and E-selectin (keeping all other atoms fixed) using the GBSW implicit solvent model[40] in CHARMM with dielectric constants equal to 80 for solvent and 1 for the solute volume, i.e., for selectin and ligand. The structure of L-selectin with the SLe^X ligand was modeled using the complex structure of P-selectin with the ligating part of PSGL-1 (PDB id 1G1S)[11] as a template.

Modeling Structures of Selectin in Complex with SLe^X Ligand. The complex structure for P-selectin with SLe^X was taken from the co-crystallized P-selectin structure 1G1S.[11] The structure of E-selectin with SLe^X was built from 1G1T[11] inserting the SLe^X conformation from 1G1S[11] (see previous section) and pulling Asn83 and Glu88 toward their positions in 1G1S.[11] To model the structure of L-selectin with SLe^X, we also used P-selectin with PSGL-1 ligand (PDB id 1G1S)[11] as a template. Here, the salt-bridge between sialic acid and $Arg97_{L\text{-}selectin}$ was forced to form by a pulling procedure with subsequent local energy minimization. For the sake of comparison, electrostatic binding energies were also calculated using the crystal structures soaked with the SLe^X ligand for P-selectin 1G1R[11] and E-selectin 1G1T.[11]

Structures of mutated selectins were generated from the corresponding adjusted and geometry-optimized wild-type structures as described above. To obtain the structure of mutant selectins, only the mutated residue and adjacent residues were pulled and energy minimized, while all other atoms were kept fix. An overview of all (crystal and model) structures used for electrostatic energy computations can be found in Table S1 of the Supporting Information.

Free Energy of Selectin Ligand Binding. The binding free energy of selectin and its ligand is governed by entropic and enthalpic contributions of the free and bound ligand. The entropy contributions upon binding are due to (1) changes in the conformational entropy of ligand, and selectin, (2) loss in translational and rotational freedom of the ligand, and (3) difference in solvent entropy if selectin and ligand are free or bound. The latter refers to the hydrophobic effect and is roughly proportional to the change in solvent accessible surface area (SASA). While the first two factors are unfavorable for binding, the latter enhances the binding affinity for hydrophobic moieties. These factors may largely cancel out. Furthermore, since the geometries of the binding pockets of the three selection types are very similar, the entropy contributions to the binding of the same ligand will hardly differ.

Enthalpic contributions consist mainly of differences of (1) electrostatic and (2) van der Waals (vdW) interactions of selectin and ligand immersed in solvent versus interactions between selectin and ligand. A third influence is due to (3) conformational enthalpy differences between free and bound selectin and ligand. This bonded part of molecular energy involves bond length, bond angle, and torsion angle energy terms. The vdW interactions between solvent and solute will be larger in the case of unbound selectin and ligand than for the bound state. However, this difference will be compensated in the bonded case by additional vdW interactions between selectin and ligand. From all entropic and enthalpic energy contributions mentioned above, the electrostatic energy is most specific and dominant for charged and polar molecular systems like selectins and their ligands. In contrast to the other enthalpic contributions, the electrostatic energy can vary significantly for different selectins and ligands. Hence, it is in particular the electrostatic energy which can explain residue specific changes in binding free energies of different selectin mutants and different ligands.

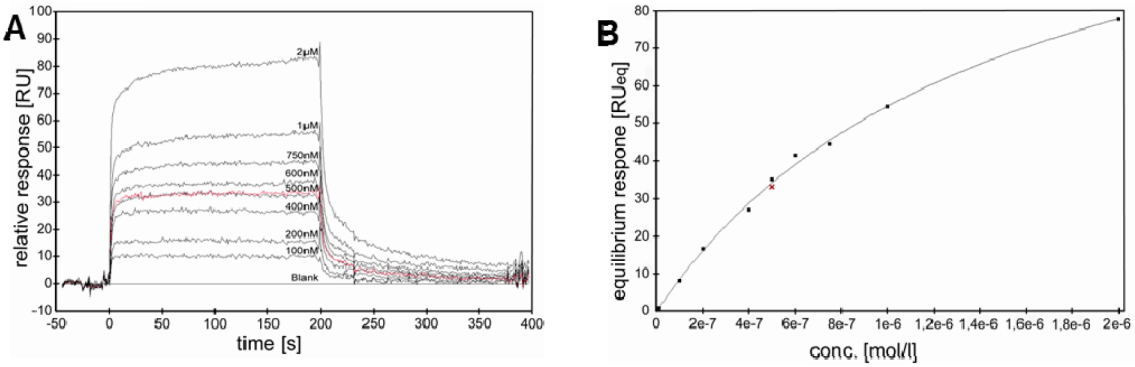

Figure 2. (A) SPR sensorgram overlay and (B) corresponding Langmuir binding isotherm of L-selectin K85A binding to SLe^X-TyS-PAA. Binding at 500 nM was determined twice. See the red curve in part A for the second run and the red cross in the binding isotherm.

Computation of Electrostatic Energy of Selectin Ligand Binding. The electrostatic energy differences between the bound and unbound state of the selectin ligand complexes were determined by numerically solving the linearized Poisson−Boltzmann equation using the program APBS.[41] The largest error source of this electrostatic energy approach is due to uncertainties of the underlying molecular structure. A more detailed discussion of this issue can be found in ref 42. The dielectric constants were set to $\varepsilon_{solvent} = 80$ for the solvent and to $\varepsilon_{protein} = 4$ inside the solute volume. The latter value compensates for moderate structural flexibility of the protein−ligand complex that is not accounted for in an electrostatic energy computation based on a few conformations only. The dielectric constant $\varepsilon_{protein} = 4$ yielded good results for electrostatic energy based computations of pK_a[25] and redox potentials[43] in proteins. Therefore, we used this value of the protein dielectric constant also in this application. To obtain reliable results, the finest grid spacing was set to 0.2 Å. The ion concentration was set to 0.0. For ion concentrations up to 1 mol/L, the electrostatic binding energies decrease by up to a few kJ/mol, but the conclusions are not affected. All atomic charges and radii were extracted from the CHARMM22 force field[20,21] parameters described above except for the calcium ion radius, where we used 1.73 Å to fit the measured solvation free energy of 380.8 kcal.[44]

The computed binding energies of selectin ligand complexes based on the electrostatic approach are compared with experimental data based on measured K_D values. From K_D, one can compute the binding free energy difference under "standard conditions"; i.e., reactants and products are at a concentration of $c_0 = 1$ mol/L (see also ref 45), which is high enough that entropy contributions occurring at low concentrations can be neglected, yielding

$$\Delta G = k_B T \ln(K_D/c_0) \quad (1)$$

The unbound reference state used in ΔG is the free selectin and ligand in a dielectric continuum with $\varepsilon_{solvent} = 80$ and $\varepsilon_{solute} = 4$.

The continuum dielectric medium used for the volumes of protein, ligand, and solvent accounts for entropy effects connected with structural variations. Hence, the computed electrostatic energies include not only enthalpic but also entropic contributions. However, since the considered entropy contributions are not complete, we prefer to use the notion of "binding energy" instead of binding free energy when we address computed electrostatic energies.

Electrostatic energy evaluations are also employed to determine the actual protonation pattern for the unbound selectin and selectin with bound ligand. The software karlsberg+[24,25] was used as in previous applications[43,46] to compute the pK_a values of titratable residues in selectin and the PSGL-1 ligand. To analyze ligand binding in more detail, the binding of individual monosaccharides was studied using the atomic partial charges from the corresponding tetrasaccharide ligand. Analogously, the binding of SLe^X to selectin was studied in the absence of one of the two terminal saccharides Fuc and SiA using for the remaining polysaccharide with the same atomic partial charges as in SLe^X.

Preparing L-Selectin Mutants. Mutations were introduced via site-directed mutagenesis using mismatch primers (metabion, Martinsried, Germany): R46A forward: 5′-ACTC-TGCCTTTCA GTGCCTCTTACTACTGGATAGG-3′, reverse: 5′-CCTATCCAGTAGTAAGAGGC ACTGAAAG-GCAGAGT-3′; K85A forward: 5′-GGTGAGCCCAACAACA-AGGC CAACAAGGAGGACTGCGTG-3′, reverse: 5′-CACGCAGTCCTCCTTGTTGGCC TTGTTGTTGGGC-TCACC-3′; E88D forward: 5′-CCCAACAACAAGAAGAACA AGGATGACTGCGTGGAGATCTATATC-3′, reverse: 5′-GATATAGATCTCCACGC AGTCATCCTTGTTCTT-CTTGTTGTTGGG-3′; D107E forward: 5′-GGCAAATGGA ACGATGAGGCCTGCCACAAACTAAAG-3′, reverse: 5′-CTTTAGTTTGTGGCAG GCCTCATCGTTCCATT-TGCC-3′. A recombinant soluble L-selectin comprising the EGF-like domain, the lectin domain, and a 6x His tag[47] cloned into a pcDNA3 vector (Invitrogen, Carlsbad, CA, USA) was used as the template. Proteins were purified with Ni-NTA resin (Qiagen, Hilden, Germany) from a conditioned medium of transfected HEK 293F cells (Gibco, Carlsbad, CA, USA). Protein was stored at −20 °C. After digestion with PNGaseF (NEB, Frankfurt, Germany), protein was purified by Ni-NTA chromatography and finally buffered to 20 mM HEPES, pH 7.4, 150 mM NaCl, and 1 mM $CaCl_2$ right before SPR measurement (SDS-PAGE of digestion shown in Figure S6 of the Supporting Information).

Surface Plasmon Resonance Studies. SPR studies were performed at 25 °C with a BIAcore X device (GE Healthcare, Freiburg, Germany). All solutions were passed through a 0.2 µm filter, degassed, and equilibrated to room temperature prior to use. Biotinylated ligands were coupled to a streptavidin (SA) chip. *N*-Acetyl-lactosamine linked to a biotinylated polyacrylamide (bio-PAA) backbone was used as a reference. Sialyl-$Lewis^X$ with (SLe^X-TyS-PAA) and without (SLe^X-PAA) sulfated tyrosines linked to bio-PAA were used as ligands. Both reference and ligands were coupled to the SA chip, yielding a baseline shift of approximately 150 resonance units (RU).

Measurements were performed at a flow rate of 30 µL/min with 20 mM HEPES, pH 7.4, 150 mM NaCl, 1 mM $CaCl_2$, and

dx.doi.org/10.1021/jp4099123 | J. Phys. Chem. B 2013, 117, 16443−16454

0.05% Tween-20 as a running buffer. Data on equilibrium binding were analyzed by nonlinear curve fitting of the Langmuir binding isotherm to the primary data using BIAevaluation software (GE Healthcare, Freiburg, Germany). For several L-selectin mutants, where no ligand binding affinity is available, SPR measurements were performed. Experimental data for a typical example are shown in Figure 2. All other measurements are shown in Figure S7 of the Supporting Information.

RESULTS AND DISCUSSION

Overview of Selectin Ligand Interaction. *Available Knowledge on Selectin Ligand Binding.* Structures of P-selectin co-crystallized with the PSGL-1 ligand show the ligand binding mode (Figure 1A).[11] The PSGL-1 ligand consists of an SLe^X motif and a polypeptide with three sulfated tyrosines (TyS) 46, 48, and 51 (Figure 1A), where TyS46 is not resolved in the crystal structure. The SLe^X motif forms several hydrogen bonds with P-selectin, and specifically, the fucose ligates the calcium ion in P-selectin. TyS48 and TyS51 of PSGL-1 are pointing into the binding interface, forming salt-bridges with P-selectin. In the same work,[11] crystal structures of P- and E-selectin soaked with the SLe^X tetrasaccharide were analyzed. Accordingly, the SLe^X ligands bind in the same pocket of the selectins but the binding geometry differs in detail from the co-crystallized structures. Unfortunately, to date, only an unbound crystal structure is available for L-selectin.[17]

Experimental binding affinities were measured with different methods, namely, nuclear magnetic resonance (NMR),[12] SPR,[13,15] or monitoring changes in intrinsic fluorescence.[14] The obtained values depend on the type of measurement, as can be seen by the different values for P-selectin binding to PSGL-1 (Figure 3). However, this does not qualitatively change which selectin is the stronger or weaker binder.

SPR Data of the Present Study. Using SPR, we determined K_D values for wt L-selectin and several point mutants (Figure 4) to validate our key results from electrostatic energy calculations, which are discussed in the following sections. The D107E mutant of L-selectin shows no significant difference in K_D value for binding to the PSGL-1 ligand analogue SLe^X-TyS-PAA. The D107E point mutation should affect SLe^X binding, which might be hidden, due to the strong interaction of L-selectin with TyS. Therefore, we also determined the K_D values for wt and D107E L-selectin binding to SLe^X-PAA.

Protonation Pattern of Selectin and Selectin Ligand Complexes. Using the computer program karlsberg+,[24,25] the protonation states of the charge variable residues in the selectins and ligands were determined as a function of pH. All titratable residues of the selectin ligand complexes are for moderate pH values (between 5 and 8) in the standard protonation state; i.e., acidic groups (Glu, Asp, C-ter) are deprotonated, basic groups (Arg, Lys, N-ter) are protonated, and all cysteines are engaged in disulfide bonds. However, the histidines adopt different protonation states in the three selectins (Table S3 of the Supporting Information). They do not change the protonation state with ligand binding, except for His114, which is only present in P-selectin. According to the titration with karlsberg+,[24,25] the pK_a of His114 in P-selectin is 6.0 in the unbound state, since it is solvent exposed. Its pK_a increases to 15.4 if P-selectin is bound to the PSGL-1 ligand. This pK_a shift is due to the formation of a salt-bridge with TyS48 of the PSGL-1 ligand. Therefore, at pH 7.6, which was the buffer condition for this particular K_D measurement,[14]

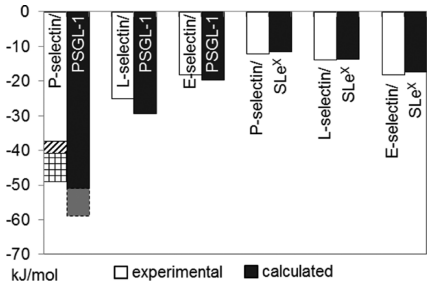

Figure 3. Binding free energies for six selectin ligand complexes in units of kJ/mol. Comparison of experimental (white bars) and theoretical values (black bars), based on electrostatic energy computations for the three types of selectins with the ligand portion of PSGL-1 or only SLe^X. Numerical values of the energies are given in Table S3A of the Supporting Information. For P-selectin, the structure co-crystallized with the ligand portion of PSGL-1 is used (PDB id 1G1S).[11] Small structural changes of the crystal structure were made to adjust H-bonds that are too short and calcium-to-ligand atom distances that are too long (see the Materials and Methods section). The gray box below the black bar indicates loss in binding energy considering the protonation of His114 (see text for explanation). For L-selectin, only a crystal structure without ligand is available (PDB id 3CFW). This structure was used to model the selectin ligand complex analogously to the co-crystallized P-selectin PSGL-1 ligand structure. For E-selectin, only a crystal structure soaked with the SLe^X ligand portion (PDB id 1G1T) is available. The P-selectin structure soaked with SLe^X differs considerably from the corresponding co-crystallized structure within the variable loop (residues 83−89; green band in Figure 1). Hence, the E-selectin complex structure was also modeled using the P-selectin structure co-crystallized with PSGL-1 ligand as a template. Experimental data for binding are taken from refs 12−15. For P-selectin binding to PSGL-1, different measured K_D values are available indicated by the different heights of the bar (white bar: data from SPR,[13] dashed and squared parts refer to different glycosylation procedures measured by intrinsic fluorescence changes[14]). No measured binding free energies are available for E-selectin with the whole ligand portion of PSGL-1. Since E-selectin binding to PSGL-1 is unaffected by removal of tyrosine sulfation,[38,39] we used the same experimental binding free energy as that for the SLe^X ligand alone.

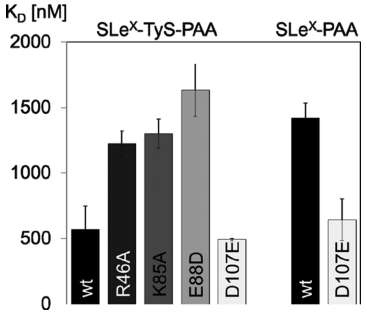

Figure 4. K_D values of L-selectin binding with ligand SLe^X-TyS-PAA (left side) and with ligand SLe^X-PAA (right side) obtained from SPR. The standard error of mean based on three to four measurements is also given. The Student's t test yields $P < 0.01$ for SLe^X-TyS-PAA with wt/R46A and wt/E88D and $P < 0.05$ for SLe^X-TyS-PAA with wt/K85A and for SLe^X-PAA with wt/D107E.

His114 is deprotonated in the unligated and protonated in the ligated P-selectin. Hence, protonation of His114 is a prerequisite of PSGL-1 binding to P-selectin and requires an additional energy of 8.0 kJ/mol at pH 7.6.

Electrostatic Contribution to Selectin Ligand Binding. We calculated the electrostatic contributions to the binding free energies of all three selectins (E-, L-, and P-selectin) with the

dx.doi.org/10.1021/jp4099123 | J. Phys. Chem. B 2013, 117, 16443−16454

PSGL-1 ligand part and SLe^X using APBS[41] to solve the Poisson equation. The structures used for the computations are based on crystal structures if available and if necessary supplemented by modeling as explained in the Materials and Methods section. The measured binding free energies are derived from K_D values,[12−15] eq 1.

The computed electrostatic binding energies correlate well with the measured binding free energies (Figure 3). Notably, computed and measured binding affinities show consistently the same trends. P-selectin is the strongest and E-selectin the weakest PSGL-1 binder. SLe^X is bound generally with lower affinity than PSGL-1. The SLe^X binding affinity is lowest for P-selectin and highest for E-selectin.

The binding energies of P- and L-selectin with PSGL-1 ligand are overestimated by theory. In P-selectin, there is a histidine at residue position 114 (His114) not present in the other two types of selectins. For the electrostatic energy computations, we initially considered His114 to be protonated for the ligated and unligated P-selectin (black bar including gray extension in Figure 3). The overestimated binding affinity of P-selectin with the PSGL-1 ligand can in part be explained, since His114 is deprotonated for the unligated P-selectin (see above). To account for this protonation change, we subtract energy costs of 8.0 kJ/mol from the binding energy, which is needed to protonate His114 in P-selectin without ligand at pH 7.6 (corresponds to removing the gray portion of the black bar in Figure 3). Including this correction, all calculated values are in close agreement with experiments. The variation of measured binding affinities found for P-selectin with PSGL-1 ligand (Figure 3) is larger than the deviations between experiment and theory.

For validation of our modeling procedure, we did electrostatic energy computations based on time frames of short molecular dynamics (MD) simulations for 10 ns each using the program CHARMM[19] (see the Supporting Information, Figures S8 and S9). We performed the calculation for the most and least well-determined complex geometry; P-selectin co-crystallized with PSGL-1 ligand and L-selectin, which was crystallized without ligand. The electrostatic binding energies from MD simulation time frames differ by less than 10% from results with the corresponding static modeled structures for P- and L-selectin bound with PSGL-1. For P- and L-selectin bound to SLe^X, the electrostatic energy differences using MD simulation time frames or the static modeled structure are slightly larger and differ by about 6 kJ/mol. This may be caused by the less well-defined force field for carbohydrates.

Interaction of Selectin with the Sialyl-Lewis^X Ligand Part. *Previous Experimental Knowledge.* The enzyme fucosyltransferase-VII performs post-translational modifications on C-R attaching saccharide moieties also at PSGL-1. These were shown to be essential for the binding ability of C-R to all three types of selectins.[48−50] Indeed, fucose—the branching saccharide monomer of SLe^X (see Figure 1B)—forms several strong non-covalent interactions with three acidic amino acids of the selectins surrounding or ligating the calcium ion and with calcium itself (see Figure 5). Two of these amino acids (Glu80, Glu88) ligating Ca^{2+} are conserved between the three types of selectins. At position 107, a glutamate (Glu107) in P-selectin and E-selectin forms a H-bond with the OH-group at position 3 of fucose (marked green in Figure 5). At the same position in L-selectin, there is an aspartate (Asp107) that cannot directly interact with fucose due to its shorter side chain.

Selectin Interaction with Different Saccharide Components of Sialyl-Lewis^X. To explore the individual contributions

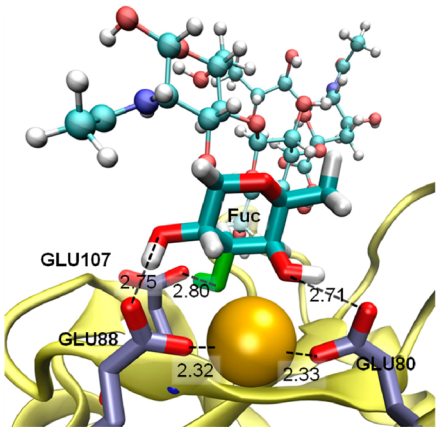

Figure 5. Binding mode of selectin with the terminal fucose monomer (Fuc) of the SLe^X motif, shown for E-selectin (PDB id 1G1T), where SLe^X was modeled using P-selectin (PDB id 1G1S)[11] as a template. The fucose ligates the Ca^{2+} ion and forms simultaneously H-bonds with three glutamates. Two of them (Glu80, Glu88) are also ligands of the Ca^{2+} ion, while Glu107 is not. The OH-group at position 3 of Fuc forming an H-bond with Glu107 is marked in green. The H-bond lengths and the distances of ligands to the Ca^{2+} ion (orange sphere), indicated by dashed lines, are given in Å.

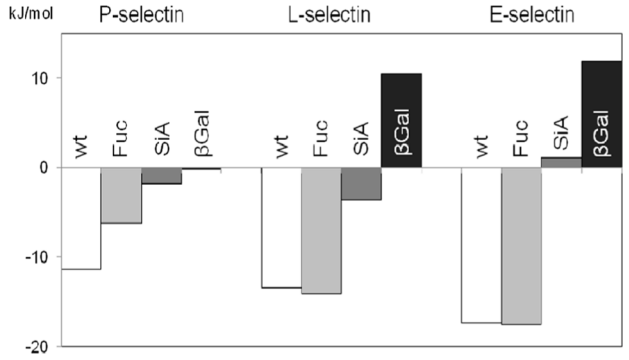

Figure 6. Calculated binding energies (kJ/mol) for selectin complexes with the wild type (wt) tetrasaccharide (SLe^X) ligand and parts of it: terminal fucose only (Fuc), sialic acid only (SiA), and β-galactose only (βGal). The precise numerical values of the energies are given in Table S3B of the Supporting Information. The binding energies for the monosaccharides were computed with the same atomic partial charges that they have within the tetrasaccharide.

to binding affinity, electrostatic interaction energies of the different SLe^X subunits with selectin were computed (results in Figure 6). All three selectins bind the fucose (Fuc) monomer with the same composition of residues in the direct neighborhood (Glu80, Glu88, and calcium), except for residue 107, which is for P- and E-selectin Glu107 and for L-selectin Asp107—whose influence is discussed below. From our calculations, we infer that fucose alone binds approximately as strong as the entire SLe^X structure in the case of L- and E-selectin and slightly weaker for P-selectin. Accordingly, the strength of fucose binding (Fuc) corresponds to the overall SLe^X binding with P-selectin being the weakest and E-selectin being the strongest binder.

The sialic acid (SiA) subunit of SLe^X interacts with the SiA binding loop 97−100 of selectin (dark blue in Figure 1A and Figure S1 of the Supporting Information). This loop possesses a sequence pattern, which is very similar in L- (RNKD) and E-selectin (REKD) but different in P-selectin (SPSA). In L- and

dx.doi.org/10.1021/jp4099123 | J. Phys. Chem. B 2013, 117, 16443−16454

E-selectin, Arg97 forms a salt-bridge with the carboxyl group of SiA, which is not possible for P-selectin. Nevertheless, the binding energy for the complex of SiA with P- or E-selectin is negligible, being even slightly positive for the E-selectin complex (Figure 6). The SiA subunit binds most strongly to L-selectin with an energy of −3.6 kJ/mol. This finding is in qualitative agreement with experiment, since treatment with neuraminidase removing SiA from SLe^X decreases binding to P- and E-selectin, while L-selectin binding becomes undetectable.[51]

β-galactose (βGal) of SLe^X forms only one H-bond with the conserved Glu92 for the three types of selectins. As a consequence, the computed electrostatic binding energy of monomeric galactose vanishes for P-selectin or is even repulsive in the case of L- and E-selectin (Figure 6). It is interesting to note that, for the P-selectin complex, Fuc, SiA, and βGal have a cumulative binding effect, while, for L- and E-selectin, Fuc clearly dominates the binding energy and βGal alone would even be repulsive.

Interaction of Glu107 in Selectin with Fucose in Sialyl-Lewis^X Ligand. The amino acids forming H-bonds with fucose are identical in P-, L-, and E-selectin except at residue position 107. In P- and E-selectin, Glu107 forms an H-bond with the OH-group at position 3 of fucose (marked green in Figure 5). This is not possible for L-selectin. It has an aspartate at position 107, whose side chain is too short to form an H-bond. As an alternative, the OH-group 3 of fucose forms an H-bond with Glu88 in L-selectin. This fucose conformation is expected to be less stable, since two OH-groups of fucose have to share the same H-bond partner Glu88. As a consequence, the binding affinity of SLe^X with L-selectin mutant D107E should be larger than with wt L-selectin. Alternatively, mutating E107D in P- and E-selectin should diminish the binding affinity to SLe^X. These effects are indeed observed in electrostatic computations of the binding energies (Figure 7).

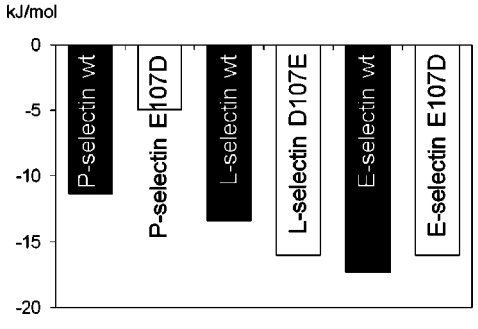

Figure 7. Electrostatic binding energy of SLe^X with the three types of selectins considering at position 107 glutamate (E107) and aspartate (D107). The wild type (wt) selectins contain E107 for P- and E-selectin and D107 for L-selectin. The precise numerical values of the energies are given in Table S3C of the Supporting Information. For the wt selectins, we use the crystal structures (P-selectin, PDB id 1G1S; L-selectin, PDB id 3CFW; E-selectin, PDB id 1G1R). For L- and E-selectin, the fucose ligand is modeled using the co-crystallized structure of P-selectin. The atomic coordinates of residue 107 and adjacent residues in the mutated selectins were modeled.

Ligand binding studies of wt L-selectin and D107E mutant using SPR showed no significant difference in binding strength for the sulfated biligand SLe^X-TyS-PAA (Figure 4). This may be due to dominant electrostatic interactions of L-selectin with TyS.[52] As can be seen, SPR binding studies of L-selectin with the monoligand SLe^X-PAA differ significantly and show larger binding affinity, when aspartate is substituted by glutamate (D107E) at residue position 107 (Figure 4).

Comparison of Co-Crystallized and Soaked Structures of Selectin Ligand Complexes. In the crystallographic studies of Somers et al.,[11] the structures of different selectin ligand complexes have been solved. P-selectin was co-crystallized with the glycosylated and tyrosine-sulfated PSGL-1 ligand (1G1S). In addition, for P- (1G1R) and E-selectin (1G1T), preformed crystals were soaked with the SLe^X ligand. The soaked and co-crystallized complex structures exhibit a very similar binding geometry for SLe^X except for the variable loop (green band in Figure 1A). In the two co-crystallized structures (P- and E-selectin), Glu88 ligates the calcium ion and Asn83 is pointing toward solvent, while in the soaked structures the opposite is the case: Asn83 ligates calcium and Glu88 points toward solvent (Figure 8). In the

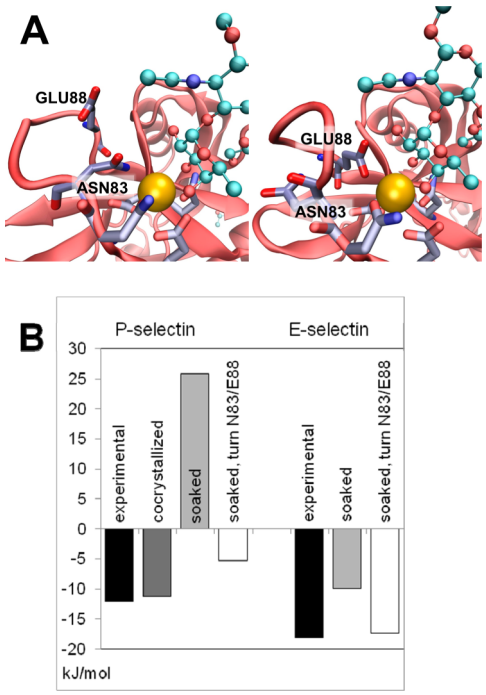

Figure 8. (A) Binding geometry of SLe^X with P-selectin for the soaked and co-crystallized complex structure. The soaked structure (left, PDB id 1G1R) exhibits Asn83 as a calcium (orange sphere) ligand with Glu88 pointing toward the solvent. The co-crystallized structure (right, PDB id 1G1S) shows Glu88 as a calcium ligand and Asn83 is pointing toward the solvent. (B) Electrostatic binding energies, comparison for the soaked and co-crystallized crystal structures of P- (PDB id 1G1R and 1G1S) and E-selectin (PDB id 1G1T) with the SLe^X ligand. Shown are also the computed binding energies based on the soaked structure with a remodeled variable loop as described in the main text (white bars). The computed binding energies are given in Table S3D of the Supporting Information.

co-crystallized selectin structure, the Ca^{2+} ligating Glu88 forms simultaneously a tight H-bond with fucose, which is not possible in the soaked crystal structure, since the corresponding Ca^{2+} ligand Asn83 cannot form the H-bond with fucose. It should be noted that both Asn83 and Glu88 are conserved among all types of selectins. Moreover the whole calcium binding pocket is mostly conserved in sequence and structure.

Binding Affinity Based on Co-Crystallized and Soaked Structures of Selectin Ligand Complexes. The calculated

dx.doi.org/10.1021/jp4099123 | J. Phys. Chem. B 2013, 117, 16443−16454

electrostatic binding energies differ largely for the co-crystallized (1G1S) and soaked (1G1R) structures of P-selectin with bound SLe^X (Figure 8B). For the co-crystallized structure, the calculated binding energy well matches the experimental value, while the computed binding energy is strongly repulsive if evaluated on the soaked complex. To determine whether this difference is only caused by the variable loop conformation, we remodeled the soaked structure (1G1R) by reorienting Asn83 and Glu88 to match the co-crystallized geometry. This modeling step decreased the binding energy by more than 30 kJ/mol (Figure 8B). Therefore, the main difference in binding strength between co-crystallized and soaked geometry seems to be the orientation of Asn83 and Glu88 and the resulting additional H-bond that fucose can form with selectin. The remaining difference in binding energy between co-crystallized and remodeled soaked structure is small and will depend on subtle structural differences.

The same remodeling strategy was applied to the E-selectin structure soaked with SLe^X using the co-crystallized P-selectin structure as a template. The difference in computed binding energies between the soaked and the remodeled soaked structure is smaller for E-selectin than for P-selectin (Figure 8B). However, bending the variable loop to allow the H-bond between Glu88 and fucose further decreases the binding energy for E-selectin with SLe^X by about 7 kJ/mol, leading to a nearly perfect agreement with the corresponding measured binding affinity. These results clearly demonstrate that only the co-crystallized complex structure (1G1S) exhibits the correct binding geometry for the variable loop, while both soaked crystal structures (1G1R and 1G1T) show P- and E-selectin in a conformation not appropriate for ligand binding.

Interestingly, the ligand-free L-selectin crystal structure (3CFW) exhibits the variable loop in a conformation similar to the co-crystallized and not to the soaked structure. This can be explained by analyzing the L-selectin crystal structure, where a mannose subunit from the glycosylated tail of a neighboring L-selectin molecule binds at the fucose binding site (see Figure S5 of the Supporting Information). For this reason, L-selectin shows the SLe^X-binding geometry, although the crystallization batch did not include ligands explicitly. The ability of L-selectin to bind to the glycosylation motif from a second L-selectin may render proper binding of SLe^X to L-selectin difficult in crystallographic essays. This could explain the reason why to date a structure of L-selectin co-crystallized with SLe^X or PSGL-1 ligand is not available.

From this, we may even conclude that in general selectins can exhibit the SLe^X binding geometry with Glu88 ligating calcium if crystallized in the presence of carbohydrate monomers that can fit into the fucose binding pocket (1G1S and 3CFW). Conversely, selectins crystallized in the absence of such carbohydrates (1G1R and 1G1T) show a non-binding geometry with Asn83 ligating calcium and Glu88 solvent exposed. This observation suggests that for the unbound lectin domain in solution the resting structure has Asn83 ligating to Ca^{2+}, while Glu88 is solvent exposed and the reorientation of Asn83 and Glu88 is induced by carbohydrate binding. Indeed, according to electrostatic solvation energies, the uncomplexed lectin domain of P-selectin is energetically more favorable by 65.6−67.2 kJ/mol in the conformation with Asn83 ligating calcium (PDB id's 1G1Q and 1G1R) than in the conformation with Glu88 ligating calcium (PDB id 1G1S). The large conformational change of reorienting Asn83/Glu88 is not possible in a preformed selectin crystal. Therefore, selectin ligand structures obtained by soaking SLe^X cannot provide the correct complex structure.

The functional relevance of the soaked selectin ligand structure can be verified experimentally, creating a mutant selectin with the conservative point mutation E88D. If the soaked crystal structures had the correct geometry for SLe^X binding, the binding affinity for this selectin mutant would differ only marginally compared to wild-type selectin, since Glu88 points toward solvent in the soaked structure. This experiment was performed with L-selectin, whose expression is established in our laboratory. Since in all three selectin types the variable loop residues Asn83 and Glu88 are conserved, one can expect the same behavior of the loop for all three types of selectins. Indeed, SPR binding studies of L-selectin showed a clear reduction of binding affinity with SLe^X-TyS-PAA (the PSGL-1 ligand analogue), when wt Glu88 was converted to Asp88 (Figure 4). This result corroborates that the geometries of the SLe^X binding pocket in the soaked crystal structures of selectin are not appropriate for ligand binding.

Interaction of Selectin with the Peptidic Part of PSGL-1 Ligand. *Structural Details.* Besides glycosylation, the N-terminus of PSGL-1 is characterized by a large negative net total charge and by post-translationally modified tyrosines 46, 48, and 51 that are sulfated. This glycosylated and sulfated N-terminal peptide loop of PSGL-1 ligand was co-crystallized with P-selectin resolving the structure of the amino acids 46−59 of PSGL-1 (PDB id 1G1S).[11] Crystal structures of PSGL-1 in complex with L- and E-selectin are not available. Therefore, they were modeled analogously to the P-selectin complex structure (see the Materials and Methods section). The interface between the binding loop of the peptidic part of PSGL-1 and selectin is mainly characterized by salt-bridges that form between the three tyrosine sulfates of PSGL-1 and positively charged amino acids of selectin. In the following, their influence on the electrostatic contribution of the binding energy is analyzed in detail.

The atomic coordinates of TyS46 were not resolved in the co-crystallized structure of P-selectin, suggesting that TyS46 is disordered. The modeled structures of TyS46 show optional salt-bridges with Lys8 and Lys112, which are solvent-exposed and thus probably unstable (see Figure S2 of the Supporting Information). In E-selectin, there is a negatively charged glutamate at residue position 8, which interacts repulsively with TyS46.

In contrast to TyS46, TyS48 is mainly not solvent exposed. In P-selectin, TyS48 forms a strong salt-bridge with His114 with an O−N distance of 2.72 Å (Figure 9). According to electrostatic energy computations with karlsberg+,[24,25] this histidine is protonated, if the PSGL-1 ligand is bound (see discussion on protonation pattern at the beginning of the Results and Discussion section). In L- and E-selectin, there is no histidine at position 114 such that the environment of TyS48 differs from P-selectin complexed with ligand. For L-selectin with modeled ligand, TyS48 forms a salt-bridge with Arg46. In the modeled structure with E-selectin, TyS48 has no salt-bridge partner and can accept only H-bonds from the polar hydrogen of Ser47 (see Figure 9).

In the crystal structure of P-selectin soaked with SLe^X (PDB id 1G1R), the variable loop points toward the solvent. By contrast, in the P-selectin structure co-crystallized with the binding portion of PSGL-1 (PDB id 1G1S), the variable loop (magenta band in Figure 1A) reaches in the selectin ligand interface and allows a salt-bridge to be formed between Arg85 and TyS51 (Figure S3 of the Supporting Information). In L-selectin, Arg85 is replaced by lysine. Therefore, we expect

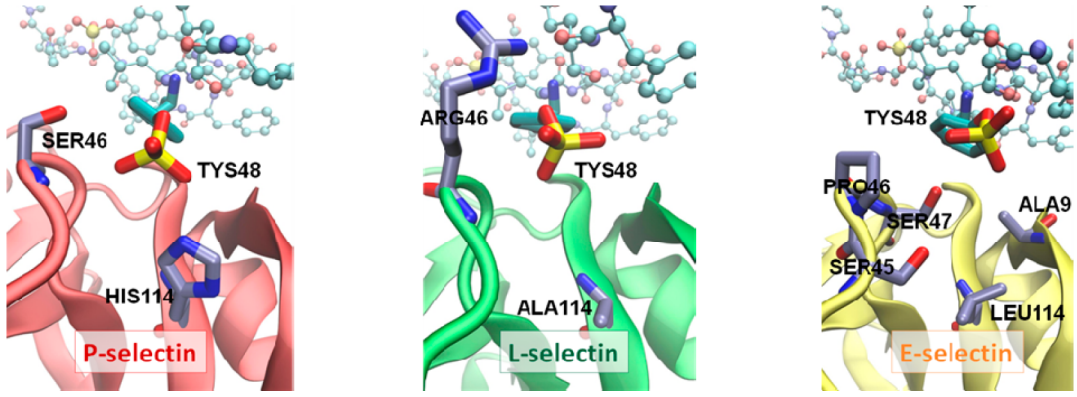

Figure 9. Binding modes of TyS48 with the three types of selectins. Left part: crystal structure of P-selectin (PDB id 1G1S, red). The displayed structures of L- (middle, green) and E-selectin (right, yellow) are modeled on the basis of the co-crystallized structure of P-selectin. TyS48 forms a salt-bridge with His114 of P-selectin and Arg46 of L-selectin. E-selectin has no potential salt-bridge partner within the corresponding protein neighborhood.

that for L-selectin complexed with ligand an analogous salt-bridge forms between TyS51 and Lys85. To enable the formation of this salt-bridge, the outward pointing variable loop in the L-selectin crystal structure without ligand (PDB id 3CFW) is replaced by the variable loop conformation present in the complex of P-selectin with ligand. With this adjusted variable loop, the electrostatic free energy of binding between L-selectin and PSGL-1 is by 13 kJ/mol more negative than with the original variable loop conformation of L-selectin crystallized in the absence of a ligand. The resulting increase in binding affinity confirms our modeling procedure with respect to the variable loop.

In E-selectin, a charge neutral glutamine is at position 85 of the variable loop and two basic residues Arg84 and Lys86 are at the next positions. However, attempts to model a firm salt-bridge between TyS51 and Arg84 or Lys86 were unsuccessful. In all cases, the distance between nitrogen (of Arg84 or Lys86) and oxygen (of TyS51) exceeded 4 Å (Figure S3 of the Supporting Information). Nevertheless, forcing the side chain of Lys86 or Arg84 to lay in the selectin ligand interface, the computed binding energy decreased by 16 or 11 kJ/mol, respectively, but the binding partners were still repulsive (Table S3F of the Supporting Information).

Selectin Interaction with Different Components of the PSGL-1 Peptide. We have systematically investigated the influence of the tyrosine sulfate salt-bridges on the binding energies of selectin ligand complexes for P- and L-selectin replacing either one or both of the salt-bridge binding partners with alanine residues (Figure 10). Our findings correlate well with the results from a fluorescence-based solid phase assay, where binding of different versions of a PSGL-1 model peptide to L- and P-selectin was analyzed.[53] Replacing TyS46 with alanine results in a moderate decrease of the computed binding energy between PSGL-1 and L- or P-selectin. Removing the sulfation at TyS46 of PSGL-1, the fluorescence-based study showed only a slight decrease in binding affinity by about a factor of 2 for both P- and L-selectins,[53] which corresponds to a 1.7 kJ/mol decrease in binding free energy.

In our computations and the fluorescence-based assay,[53] the mutation of TyS48 or TyS51 to alanine leads to a significant decrease of the binding energy for P- and L-selectin complexed with PSGL-1 (Figure 10). However, the fluorescence data show a slighter decrease for the TyS51A mutant, while the computed binding affinities show practically the same decrease for both mutants, TyS48A and TyS51A. This may be due to structural

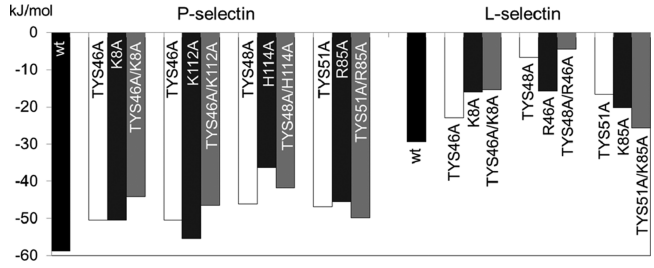

Figure 10. Influence of the salt-bridges involving the sulfated tyrosines (TyS46, TyS48, TyS51) of the PSGL-1 ligand on binding to P- and L-selectin. The electrostatic part of the binding energy is computed for the wild-type (wt) selectins complexed with the wt PSGL-1 ligand (black) and for point mutations to alanine in selectin and/or PSGL-1 ligand. Salt-bridge partners are grouped, first showing the TyS mutant in PSGL-1 ligand (white), second the mutant of the corresponding salt-bridge partner of selectin (dark gray), and third the double mutant of the salt-bridge partners (light gray). The precise numerical values of the computed energies are given in Table S3G of the Supporting Information.

rearrangements in the variable loop (Figure 1A and Figure S3 of the Supporting Information), which can be the result of point mutation.

The importance of salt-bridges between tyrosine sulfates and basic amino acids in L-selectin is also experimentally confirmed in our study. The SPR data of the L-selectin mutants R46A and K85A that eliminate the salt-bridges show a significant loss of binding strength (Figure 4).

Interaction of the Whole PSGL-1 Ligand with Selectin. In contrast to P-selectin, E-selectin binds PSGL-1 independent from sulfated tyrosines.[38,39] We compared the electrostatic binding energy of the PSGL-1 ligand bound with P- or E-selectin. For E-selectin, we compared the binding energies obtained with the PSGL-1 conformation taken from the P-selectin complex (PDB id 1G1S)[11] with an elongated PSGL-1 peptide conformation stretching into the solvent and only SLe^X attached to E-selectin (see Figure S4 of the Supporting Information for geometries). From these computations, we observed that PSGL-1 and E-selectin are strongly repulsive, if PSGL-1 is in the P-selectin conformation, while with the peptide conformation detached from E-selectin the binding energy is comparable to binding of SLe^X alone. In fact, orienting PSGL-1 bound at E-selectin analogous to the P-selectin complex,

dx.doi.org/10.1021/jp4099123 | J. Phys. Chem. B 2013, 117, 16443−16454

no adequate salt-bridge partners can be found for any of the three tyrosine sulfates, thereby explaining the repulsive interaction. Together with the binding behavior observed experimentally,[38,39] it strongly suggests that E-selectin does only bind the SLe^X saccharide and not the peptidic part of the PSGL-1 ligand.

The binding strength and kinetics of the selectin−PSGL-1 interaction are dominated by long-range electrostatic attraction via opposite charges of the interaction partners. The PSGL-1 ligand is highly negatively charged carrying a net total charge of −8 due to its three tyrosine sulfates, three glutamates, and two aspartates. Conversely, the lectin domains of P- and L-selectin have a complementary positive net total charge of +9 for P-selectin and +5 for L-selectin, while the lectin domain of E-selectin is charge neutral. These charges correlate qualitatively with the binding energies between the PSGL-1 ligand and the different selectin types.

CONCLUSIONS

The present study characterizes selectin ligand binding for all three types of selectins computing the electrostatic contributions to binding free energy by solving the Poisson−Boltzmann equation.[54] Subtle differences of these molecular systems in long-range electrostatic interactions and the involvement of saccharides constitute a challenge for theory to describe quantitatively how binding affinity depends on molecular differences of the three selectin types. Notably, available and own measurements on binding affinities were reproduced qualitatively and often even quantitatively, indicating that electrostatic interactions dominate the binding affinity of selectins with the C-R.

The selectins are mainly positively charged, while the PSGL-1 ligand carries a negative charge of −8. The net total charges of the lectin domains are +9, +5, and 0 for P-, L-, and E-selectin, respectively. These charge patterns enhance the binding affinity and kinetics of selectin ligand binding for P- and L-selectin in agreement with experiments. Due to charge neutrality, E-selectin is not capable of long-range attractive electrostatic interactions with the negatively charged peptidic part of the PSGL-1 ligand. As a consequence, the peptidic part of the PSGL-1 ligand will probably not contribute to the binding affinity with E-selectin. Accordingly, our electrostatic energy computations result only in attractive binding energies when the peptidic part of the PSGL-1 ligand is fully solvent exposed and not in contact with E-selectin. This agrees with the finding that the binding of PSGL-1 ligand to E-selectin does not depend on whether the tyrosines are sulfated or not.[38,39]

According to the present study, the crystal structures of selectin soaked with the SLe^X ligand are not appropriate to understand selectin PSGL-1 binding. They yield weak or even repulsive interactions between selectin and ligand, while model structures based on P-selectin co-crystallized with the PSGL-1 ligand (including SLe^X) yield attractive interactions in semi-quantitative agreement with measured data. The reason that the selectin structures soaked with SLe^X differ from the corresponding co-crystallized structures may likely be due to the conformation of the variable loop of selectin (magenta band in Figure 1A), which adopts a different conformation in the absence of a ligand. This difference was confirmed by SPR data in this study for the L-selectin mutant E88D. This mutant mimics to some degree the variable loop conformation of the soaked structure by effectively displacing the carboxylic acid of the variable loop away from the Ca^{2+} ion to which it is ligated in wt selectin. As a result, a lower binding affinity of E88D L-selectin to SLe^X-TyS-PAA (the PSGL-1 ligand analogue) was detected, which emphasizes the importance of the proper conformation of the variable loop.

Interestingly, a monomeric saccharide that can mimic the fucose selectin interaction like, for instance, mannose is sufficient to ensure that the variable loop is in the conformation suitable for ligand binding. This may be a useful hint to promote co-crystallization of selectin with the appropriate ligands. The analysis of the individual contributions binding SLe^X with selectin reveals that the most important contribution is due to fucose, which binds to the Ca^{2+} ion and forms three strong H-bonds with acidic groups of selectin. All three types of selectins carry a large fraction of charged residues with different compositions. The more distant charged residues contribute also to the variation of electrostatic binding energies of fucose with selectin and are likely responsible for the type specificity of binding of selectin with SLe^X ligand.

The ligand and the Ca^{2+} binding pocket of selectin are highly conserved except for position 107 with Glu in P- and E-selectin and Asp in L-selectin. Measuring the binding affinity for the mutant D107E in L-selectin shows an increase in binding affinity in the SPR experiment to the SLe^X-PAA ligand. Thus, Glu107 is probably part of the reason why E-selectin has a stronger affinity for SLe^X than L-selectin has. On the other hand, the SiA binding mode with the loop 97−100 (dark blue band in Figure 1A) is similar in L- and E-selectin but differs strongly for P-selectin, which is the weakest binder of the SiA subunit.

From the peptidic part of PSGL-1, the negatively charged sulfated tyrosines can predominantly contribute to selectin ligand binding, although the salt-bridges they form with the selectins are partly solvent exposed. Thus, especially the salt bridge to TyS46 is relatively weak, which is corroborated by the fact that atomic coordinates of the TyS46 side chain are not available in the P-selectin structure co-crystallized with the PSGL-1 ligand. SPR data of the present study confirmed that L-selectin binds to PSGL-1 in a similar mode as P-selectin, i.e., mainly via salt-bridges with tyrosine sulfates. Accordingly, the binding of the PSGL-1 ligand analogue SLe^X-TyS-PAA with the L-selectin mutants R46A and K85A is largely weakened. The only titratable residue that varies the protonation state with PSGL-1 ligand binding is His114, appearing in P-selectin only. It becomes protonated to form a salt-bridge with the sulfated TyS51, if the PSGL-1 ligand is bound.

Although the SPR data measured for the present work do not agree quantitatively with previous measurements,[12,15] they are in qualitative agreement. The difference in experimental data may have several reasons. *N*-glycosylation of L-selectin shows a broad diversity[47] and may contribute considerably to the measured binding affinity.[55,56] Its influence might have weakened binding in previous studies, resulting in larger K_D values.[12,15] Therefore, we decided to remove the glycosylation. Furthermore, the ligand presented on our SPR sensor chip differs from the natural one with respect to the degree of multivalency, which in turn alters the apparent binding affinity. Thus, presenting SLe^X and TyS together on the same PAA backbone may enhance the apparent binding affinity considerably compared to a monomeric setup, or if presented on separate PAA backbones.[52] A general concern is that the SPR technique might suffer from unspecific binding to the used chip and non-equilibrium flow-through conditions. This could affect especially weak interactions like selectin C-R binding. However, all of these inconsistencies between different experimental

setups will have the same impact on all measurements, when SPR sensor chips of the same batch are used throughout, as was done in the present study. Therefore, we have focused our discussion on the relative effects of our measurements.

In the present study, we were able to quantify the influence of the different PSGL-1 ligand and selectin components on selectin ligand binding and to verify these results with available and new experiments. The deeper understanding of selectin C-R interactions in atomic resolution, based on the present study, can foster the development of ligands that modulate these interactions, which is a fundamental issue for pharmaceutical industry. It opens the possibility to control the immune response by tuning the extravasation process of leukocytes and preventing other cell types, which mistakenly express selectins, to attach to blood vessel walls, fostering metastasis. Hence, understanding selectin C-R interaction on the molecular level can provide the basis to fight diseases in diverse fields ranging from autoimmune reactions to cancer.

■ ASSOCIATED CONTENT

Supporting Information

The biomedical background on selectins, the structures for quantum mechanical calculations, a list of all complex structures used and their binding energies, several binding geometries of interest, and detailed data of SPR measurements. This material is available free of charge via the Internet at http://pubs.acs.org.

■ AUTHOR INFORMATION

Corresponding Author

*Phone: +49 (30) 838-54387. E-mail: knapp@chemie.fu-berlin.de.

Notes

The authors declare no competing financial interest.

■ ACKNOWLEDGMENTS

We would like to thank Dr. Artur Galstyan for support in computing atomic partial charges and Dr. Arturo Robertazzi for careful proof-reading. This work has been financially supported by the German research society (DFG) with projects B7 and C1 in Sfb 765, project C2 in Sfb 1078, and a project in the research training group "Computational System Biology" (CSB). A.L.W. is grateful for receiving the Elsa-Neumann fellowship of the state of Berlin.

■ ABBREVIATIONS

β-galactose, βGal; biotinylated polyacrylamide, bio-PAA; counter-receptor, C-R; epidermal growth factor domain, EGF domain; fucose, Fuc; *N*-acetylgalactosamine, NGA; *N*-acetylglucosamine, NAG; nuclear magnetic resonance, NMR; P-selectin glycoprotein ligand-1, PSGL-1; resonance unit, RU; sialic acid, SiA; Sialyl-Lewis^X, SLe^X; streptavidin, SA; surface plasmon resonance, SPR; van der Waals interaction, vdW interaction; surface plasmon resonance, SPR; white blood cells, WBC

■ REFERENCES

(1) Ley, K.; Laudanna, C.; Cybulsky, M. I.; Nourshargh, S. Getting to the Site of Inflammation: the Leukocyte Adhesion Cascade Updated. *Nat. Rev. Immunol.* **2007**, *7*, 678−689.

(2) Bhatia, S. K.; King, M. R.; Hammer, D. A. The State Diagram for Cell Adhesion Mediated by Two Receptors. *Biophys. J.* **2003**, *84*, 2671−2690.

(3) Ley, K. The Role of Selectins in Inflammation and Disease. *Trends Mol. Med.* **2003**, *9*, 263−268.

(4) Kneuer, C.; Ehrhardt, C.; Radomski, M. W.; Bakowsky, U. Selectins−Potential Pharmacological Targets? *Drug Discovery Today* **2006**, *11*, 1034−1040.

(5) Barthel, S. R.; Gavino, J. D.; Descheny, L.; Dimitroff, C. J. Targeting Selectins and Selectin Ligands in Inflammation and Cancer. *Expert Opin. Ther. Targets* **2007**, *11*, 1473−1491.

(6) Romano, S. J.; Slee, D. H. Targeting Selectins for the Treatment of Respiratory Diseases. *Curr. Opin. Invest. Drugs* **2001**, *2*, 907−913.

(7) Fasting, C.; Schalley, C. A.; Weber, M.; Seitz, O.; Hecht, S.; Koksch, B.; Dernedde, J.; Graf, C.; Knapp, E. W.; Haag, R. Multivalency as a Chemical Organization and Action Principle. *Angew. Chem., Int. Ed. Engl.* **2012**, *51*, 10472−10498.

(8) Roskamp, M.; Enders, S.; Pfrengle, F.; Yekta, S.; Dekaris, V.; Dernedde, J.; Reissig, H. U.; Schlecht, S. Multivalent Interaction and Selectivities in Selectin Binding of Functionalized Gold Colloids Decorated with Carbohydrate Mimetics. *Org. Biomol. Chem.* **2011**, *9*, 7448−7456.

(9) Sanders, W. J.; Gordon, E. J.; Dwir, O.; Beck, P. J.; Alon, R.; Kiessling, L. L. Inhibition of L-Selectin-Mediated Leukocyte Rolling by Synthetic Glycoprotein Mimics. *J. Biol. Chem.* **1999**, *274*, 5271−5278.

(10) McEver, R. P.; Zhu, C. Rolling Cell Adhesion. *Annu. Rev. Cell Dev. Biol.* **2010**, *26*, 363−396.

(11) Somers, W. S.; Tang, J.; Shaw, G. D.; Camphausen, R. T. Insights into the Molecular Basis of Leukocyte Tethering and Rolling Revealed by Structures of P- and E-Selectin Bound to SLe(X) and PSGL-1. *Cell* **2000**, *103*, 467−479.

(12) Poppe, L.; Brown, G. S.; Philo, J. S.; Nikrad, P. V.; Shah, B. H. Conformation of sLex Tetrasaccharide, Free in Solution and Bound to E-, P-, and L-Selectin. *J. Am. Chem. Soc.* **1997**, *119*, 1727−1736.

(13) Mehta, P.; Cummings, R. D.; McEver, R. P. Affinity and Kinetic Analysis of P-Selectin Binding to P-Selectin Glycoprotein Ligand-1. *J. Biol. Chem.* **1998**, *273*, 32506−32513.

(14) Croce, K.; Freedman, S. J.; Furie, B. C.; Furie, B. Interaction between Soluble P-Selectin and Soluble P-Selectin Glycoprotein Ligand 1: Equilibrium Binding Analysis. *Biochemistry* **1998**, *37*, 16472−16480.

(15) Klopocki, A. G.; Yago, T.; Mehta, P.; Yang, J.; Wu, T.; Leppanen, A.; Bovin, N. V.; Cummings, R. D.; Zhu, C.; McEver, R. P. Replacing a Lectin Domain Residue in L-Selectin Enhances Binding to P-Selectin Glycoprotein Ligand-1 But Not to 6-Sulfo-Sialyl Lewis x. *J. Biol. Chem.* **2008**, *283*, 11493−11500.

(16) Berman, H. M.; Westbrook, J.; Feng, Z.; Gilliland, G.; Bhat, T. N.; Weissig, H.; Shindyalov, I. N.; Bourne, P. E. The Protein Data Bank. *Nucleic Acids Res.* **2000**, *28*, 235−242.

(17) Mehta, P.; McEver, R. P. Structure of Lectin and EGF Domains of L-Selectin. To be published.

(18) Brooks, B. R.; Bruccoleri, R. E.; Olafson, B. D.; States, D. J.; Swaminathan, S.; Karplus, M. CHARMM: A program for macromolecular energy, minimization, and dynamics calculations. *J. Comput. Chem.* **1983**, *4*, 187−217.

(19) Brooks, B. R.; Brooks, C. L., 3rd; Mackerell, A. D., Jr.; Nilsson, L.; Petrella, R. J.; Roux, B.; Won, Y.; Archontis, G.; Bartels, C.; Boresch, S.; et al. CHARMM: the Biomolecular Simulation Program. *J. Comput. Chem.* **2009**, *30*, 1545−1614.

(20) MacKerell, A. D.; Bashford, D.; Bellott, M.; Dunbrack, R. L.; Evanseck, J. D.; Field, M. J.; Fischer, S.; Gao, J.; Guo, H.; Ha, S.; et al. All-Atom Empirical Potential for Molecular Modeling and Dynamics Studies of Proteins. *J. Phys. Chem. B* **1998**, *102*, 3586−3616.

(21) MacKerell, A. D., Jr.; Feig, M.; Brooks, C. L., 3rd. Extending the Treatment of Backbone Energetics in Protein Force Fields: Limitations of Gas-Phase Quantum Mechanics in Reproducing Protein Conformational Distributions in Molecular Dynamics Simulations. *J. Comput. Chem.* **2004**, *25*, 1400−1415.

(22) Guvench, O.; Greene, S. N.; Kamath, G.; Brady, J. W.; Venable, R. M.; Pastor, R. W.; Mackerell, A. D., Jr. Additive Empirical Force Field for Hexopyranose Monosaccharides. *J. Comput. Chem.* **2008**, *29*, 2543−2564.

(23) Guvench, O.; Hatcher, E. R.; Venable, R. M.; Pastor, R. W.; Mackerell, A. D. CHARMM Additive All-Atom Force Field for

Glycosidic Linkages between Hexopyranoses. *J. Chem. Theory Comput.* **2009**, *5*, 2353−2370.
(24) Rabenstein, B.; Knapp, E. W. Calculated pH-dependent population and protonation of carbon-monoxy-myoglobin conformers. *Biophys. J.* **2001**, *80*, 1141−1150.
(25) Kieseritzky, G.; Knapp, E. W. Optimizing pKa Computation in Proteins with pH Adapted Conformations. *Proteins* **2008**, *71*, 1335−1348.
(26) Parr, R. G.; Yang, W. *Density-Functional Theory of Atoms and Molecules*; Oxford University Press: Oxford, U.K., 1989.
(27) Koch, W.; Holthausen, M. C. *Wie gut ist Dichtefunktionaltheorie? A Chemist's Guide to Density Functional Theory*; Wiley-VCH: Weinheim, Germany, 2000.
(28) *Jaguar*, version 7.7, 7.7; Schrödinger, LLC: New York, 2010.
(29) Vosko, S. H.; Wilk, L.; Nusair, M. Accurate Spin-Dependent Electron Liquid Correlation Energies for Local Spin-Density Calculations - a Critical Analysis. *Can. J. Phys.* **1980**, *58*, 1200−1211.
(30) Lee, C. T.; Yang, W. T.; Parr, R. G. Development of the Colle-Salvetti Correlation-Energy Formula into a Functional of the Electron-Density. *Phys. Rev. B* **1988**, *37*, 785−789.
(31) Becke, A. D. Density-Functional Thermochemistry. 3. The Role of Exact Exchange. *J. Chem. Phys.* **1993**, *98*, 5648−5652.
(32) Stephens, P. J.; Devlin, F. J.; Chabalowski, C. F.; Frisch, M. J. Ab-Initio Calculation of Vibrational Absorption and Circular-Dichroism Spectra Using Density-Functional Force-Fields. *J. Phys. Chem.* **1994**, *98*, 11623−11627.
(33) Hehre, W. J.; Ditchfield, J. A.; Pople, J. A. Self-Consistent Molecular-Orbital Methods 0.12. Further Extensions of Gaussian-Type Basis Sets for Use in Molecular-Orbital Studies of Organic-Molecules. *J. Chem. Phys.* **1972**, *56*, 2257−2261.
(34) Harihara, P. C.; Pople, J. A. Influence of Polarization Functions on Molecular-Orbital Hydrogenation Energies. *Theor. Chim. Acta.* **1973**, *28*, 213−222.
(35) Francl, M. M.; Pietro, W. J.; Hehre, W. J.; Binkley, J. S.; Gordon, M. S.; Defrees, D. J.; Pople, J. A. Self-Consistent Molecular-Orbital Methods 0.23. A Polarization-Type Basis Set for 2Nd-Row Elements. *J. Chem. Phys.* **1982**, *77*, 3654−3665.
(36) Cornell, W. D.; Cieplak, P.; Bayly, C. I.; Kollman, P. A. Application of Resp Charges to Calculate Conformational Energies, Hydrogen-Bond Energies, and Free-Energies of Solvation. *J. Am. Chem. Soc.* **1993**, *115*, 9620−9631.
(37) Bayly, C. I.; Cieplak, P.; Cornell, W. D.; Kollman, P. A. A Well-Behaved Electrostatic Potential Based Method Using Charge Restraints for Deriving Atomic Charges - the Resp Model. *J. Phys. Chem.* **1993**, *97*, 10269−10280.
(38) Sako, D.; Comess, K. M.; Barone, K. M.; Camphausen, R. T.; Cumming, D. A.; Shaw, G. D. A Sulfated Peptide Segment at the Amino Terminus of PSGL-1 is Critical for P-Selectin Binding. *Cell* **1995**, *83*, 323−331.
(39) Pouyani, T.; Seed, B. PSGL-1 Recognition of P-Selectin is Controlled by a Tyrosine Sulfation Consensus at the PSGL-1 Amino Terminus. *Cell* **1995**, *83*, 333−343.
(40) Im, W. P.; Lee, M. S.; Brooks, C. L. Generalized Born Model with a Simple Smoothing Function. *J. Comput. Chem.* **2003**, *24*, 1691−1702.
(41) Baker, N. A.; Sept, D.; Joseph, S.; Holst, M. J.; McCammon, J. A. Electrostatics of Nanosystems: Application to Microtubules and the Ribosome. *Proc. Natl. Acad. Sci. U.S.A.* **2001**, *98*, 10037−10041.
(42) Rabenstein, B.; Knapp, E. W. Problems Evaluating Energetics of Electron Transfer from QA to QB: The Light Exposed and Dark-Adapted Bacterial Reaction Center. *ACS Symp. Ser.* **2004**, *883*, 71−92.
(43) Gamiz-Hernandez, A. P.; Kieseritzky, G.; Galstyan, A. S.; Demir-Kavuk, O.; Knapp, E. W. Understanding Properties of Cofactors in Proteins: Redox Potentials of Synthetic Cytochromes b. *ChemPhysChem* **2010**, *11*, 1196−1206.
(44) Aqvist, J. Ion Water Interaction Potentials Derived from Free-Energy Perturbation Simulations. *J. Phys. Chem.* **1990**, *94*, 8021−8024.
(45) Wild, M. K.; Huang, M. C.; Schulze-Horsel, U.; van der Merwe, P. A.; Vestweber, D. Affinity, Kinetics, and Thermodynamics of E-Selectin Binding to E-Selectin Ligand-1. *J. Biol. Chem.* **2001**, *276*, 31602−31612.
(46) Kieseritzky, G.; Knapp, E. W. Charge Transport in the ClC-Type Chloride-Proton Anti-Porter from Escherichia Coli. *J. Biol. Chem.* **2011**, *286*, 2976−2986.
(47) Wedepohl, S.; Kaup, M.; Riese, S. B.; Berger, M.; Dernedde, J.; Tauber, R.; Blanchard, V. N-Glycan Analysis of Recombinant L-Selectin Reveals Sulfated GalNAc and GalNAc-GalNAc Motifs. *J. Proteome Res.* **2010**, *9*, 3403−3411.
(48) Knibbs, R. N.; Craig, R. A.; Maly, P.; Smith, P. L.; Wolber, F. M.; Faulkner, N. E.; Lowe, J. B.; Stoolman, L. M. Alpha(1,3)-Fucosyltransferase VII-Dependent Synthesis of P- and E-Selectin Ligands on Cultured T Lymphoblasts. *J. Immunol.* **1998**, *161*, 6305−6315.
(49) Maly, P.; Thall, A.; Petryniak, B.; Rogers, C. E.; Smith, P. L.; Marks, R. M.; Kelly, R. J.; Gersten, K. M.; Cheng, G.; Saunders, T. L.; et al. The Alpha(1,3)Fucosyltransferase Fuc-TVII Controls Leukocyte Trafficking Through an Essential Role in L-, E-, and P-Selectin Ligand Biosynthesis. *Cell* **1996**, *86*, 643−653.
(50) Erdmann, I.; Scheidegger, E. P.; Koch, F. K.; Heinzerling, L.; Odermatt, B.; Burg, G.; Lowe, J. B.; Kundig, T. M. Fucosyltransferase VII-Deficient Mice with Defective E-, P-, and L-Selectin Ligands Show Impaired CD4+ and CD8+ T Cell Migration into the Skin, But Normal Extravasation into Visceral Organs. *J. Immunol.* **2002**, *168*, 2139−2146.
(51) Zhang, X.; Bogorin, D. F.; Moy, V. T. Molecular basis of the dynamic strength of the sialyl Lewis X–selectin interaction. *ChemPhysChem* **2004**, *5*, 175−182.
(52) Enders, S.; Bernhard, G.; Zakrzewicz, A.; Tauber, R. Inhibition of L-Selectin Binding by Polyacrylamide-Based Conjugates Under Defined Flow Conditions. *Biochim. Biophys. Acta* **2007**, *1770*, 1441−1449.
(53) Leppänen, A.; Yago, T.; Otto, V. I.; McEver, R. P.; Cummings, R. D. Model Glycosulfopeptides from P-Selectin Glycoprotein Ligand-1 Require Tyrosine Sulfation and a Core 2-Branched O-Glycan to Bind to L-Selectin. *J. Biol. Chem.* **2003**, *278*, 26391−26400.
(54) Ullmann, G. M.; Knapp, E. W. Electrostatic Models for Computing Protonation and Redox Equilibria in Proteins. *Eur. Biophys. J.* **1999**, *28*, 533−551.
(55) Enders, S.; Riese, S. B.; Bernhard, G.; Dernedde, J.; Reutter, W.; Tauber, R. Binding Activity of Recombinant Human L-Selectin-Fc(gamma) is Modified by Sialylation. *Biochem. Eng. J.* **2010**, *48*, 253−259.
(56) Papp, I.; Dernedde, J.; Enders, S.; Haag, R. Modular Synthesis of Multivalent Glycoarchitectures and Their Unique Selectin Binding Behavior. *Chem. Commun.* **2008**, 5851−5853.